

# Adapted Approach for Omnidirectional Egomotion Estimation

A. Radgui, Mohammed V-Agdal University, Morocco

C. Demonceaux, University of Picardie Jules Verne, France

E. Mouaddib, University of Picardie Jules Verne, France

M. Rziza, Mohammed V-Agdal University, Morocco

D. Aboutajdine, Mohammed V-Agdal University, Morocco

---

## ABSTRACT

*Egomotion estimation is based principally on the estimation of the optical flow in the image. Recent research has shown that the use of omnidirectional systems with large fields of view allow overcoming the limitation presented in planar-projection imagery in order to address the problem of motion analysis. For omnidirectional images, the 2D motion is often estimated using methods developed for perspective images. This paper adapts motion field calculated using adapted method which takes into account the distortions existing in the omnidirectional image. This 2D motion field is then used as input to the egomotion estimation process using spherical representation of the motion equation. Experimental results are shown and comparison of error measures are given to confirm that succeeded estimation of camera motion will be obtained when using an adapted method to estimate optical flow.*

**Keywords:** Egomotion, Motion Model, Neighborhood, Omnidirectional Image, Optical Flow

---

## INTRODUCTION

The progress of techniques for autonomous robot navigation constitutes one of the major trends in the current research on mobile robotics (Kim & Suga, 2007; Yoshizaki et al., 2008; Wang et al., 2006; Bunschoten & Kroese, 2003; Winters et al., 2000). The objective is to make

robot able to plan its path and execute its plan without human intervention. One way to do this is to enable robot to estimate the egomotion starting with the images of environment. This estimation can, for example, be used by the robot to reconstruct the scene in three-dimensional space. The egomotion estimation problem consists in recovering the camera motion relative to the environment taking an image sequence as an input.

DOI: 10.4018/ijcvip.2011010101

In the past, different approaches are proposed to estimate motion from perspective images that only offer a limited field of view. It was also proved that estimation methods from these images have difficulty to distinguish small pure translations from small pure rotations. Recently, the developed omnidirectional cameras with large field of view have been able to overcome the limited field of view introduced by planar projections (Gluckman & Nayar, 1998). The omnidirectional images with hemispherical field of view contain global information about motion with the presence of the focus of expansion (FOE) and/or the focus of contraction (FOC) in the images. If a whole spherical field of view is offered, it is guaranteed that both FOE and FOC are in the image. Consequently, the optical flow filed analysis from omnidirectional images is more efficient also with smooth camera motion.

The process of egomotion estimation naturally consists in estimating the optical flow (Gluckman & Nayar, 1998; Vassallo et al., 2002; Shakernia et al., 2003; Lim & Barnes, 2008; Gandhi & Trivedi, 2005), or features correspondences (Svoboda et al., 1998; Lee et al., 2000; Thanh et al., 2008), and then extracting the 3D camera motion from the 2D information computed in images. In omnidirectional vision, several methods, proposed in last few years, are concerned with egomotion estimation from motion field. Gluckman and Nayar (1998) showed that good results for egomotion can be obtained by using omnidirectional images. They project the image motion on a spherical surface using Jacobians of transformations to determine motion of the camera. A different Jacobian function must be determined according to the particular projection model of the used camera. This approach was generalized later by Vassallo et al. (2002). They present general Jacobian as a function of the parameters of the central panoramic projection model that can describe a wide variety of omnidirectional cameras. In another direction, Shakernia et al. (2003) show that egomotion algorithms proposed for perspective images by Tian et al. (1996) can be directly applied to the back-projection flow.

The so-called back-projection flow is obtained by lifting the optical flow from the image plane onto a virtual curved surface instead of spherical surface to simplify the Jacobians. They showed that the unified projection model for central panoramic cameras, developed by Geyer and Daniilidis (2000), can be considered as a projection onto a virtual curved retina that is intrinsic to the camera geometry. Recently, Lim et al. in (2008) and (2009) present geometrical constraint considering the flow at antipodal points. They show that it allows estimating of direction of motion using a spherical representation of images.

Among the proposed approaches for ego-motion estimation based on features correspondences, Svoboda et al. (1998) use the detected feature to estimate the essential matrix between two frames using the 8-point algorithm. They also note that the motion estimation is more stable with omnidirectional cameras compared to the rectilinear ones. Lee et al. (2000) adapt the motion estimation method to large motions by using a novel Recursive Rotation Factorization (RRF) that removes the image motions due to rotation. Recently, Thanh et al. (2008) detect image features in omnidirectional images using a conventional feature detector and then classify it into near and far features. Rotation is recovered using far features, and then translation is estimated from near features using the estimated rotation.

All previous works, those are using the optical flow, compute egomotion from 2D motion field using classical methods. We propose to use an adapted method to the omnidirectional images to improve the estimation of the observer motion. This adapted method considers the distortion presented in omnidirectional image and allows efficient motion field and more accurate 3D motion. Like Gluckman & Nayar (1998) and Vassallo et al. (2002), we will map the vector flow in the sphere and compute rotation and direction of translation using the well known algorithm of Bruss & Horn (1983). The reminder of the paper is organized as follows. In section 1, we shall briefly present the adapted method for motion field estimation. The detail of this

technique can be found in Radgui et al. (2008). Section 2 describes the combined Brus-Horn's and Gluckman's methods for motion analysis using our adapted vectors flow. In section 3, the experimental results are given and comparative measurements are discussed for synthetic and real images. We shall eventually give our conclusion in section 4.

## 1. ADAPTED MOTION FIELD ESTIMATION

Optical flow algorithms estimate the deformations between two images. The basic assumption for the optical flow calculation is that pixel intensity is conserved. It is assumed that the intensity (or color) of objects has not significantly changed between the two images. Based on this idea, we obtain the well known optical flow constraint equation:

$$\vec{\nabla}I \cdot \vec{V} + \frac{\partial I}{\partial t} = 0 \quad (1)$$

where,  $\vec{\nabla}I = \left( \frac{\partial I}{\partial x}, \frac{\partial I}{\partial y} \right)$  is the gradient of the image.

Lucas and Kanade (1981) compute the optical flow on a point  $(x,y)$ , considering that the motion is constant in a fixed neighborhood  $V(x,y)$  of this point, as solution of:

$$\vec{V}I(x,y) = \arg \min_e \sum_{x'} y e \in \vartheta_{x,y} \left[ \frac{\partial I}{\partial x}, a + \frac{\partial I}{\partial y}, b + \frac{\partial I}{\partial t} \right]^2 \quad (2)$$

Although the constant model and the fixed neighborhood give good results for optical flow estimation in perspective cameras, these two assumptions are never verified in the omnidirectional images due to the distortions. In our previous work (Radgui, 2008), we have proposed to use new constraint based on motion model defined for paracatadioptric images and which is appropriate to the geometry of

our image formation. We give an outline of our suggested method. We have defined a new constraint for the optical flow around the point  $(x,y)$  and a new neighborhood adapted to our omnidirectional images.

### 1.1. Motion Model in Paracatadioptric Images

We consider omnidirectional sensor composed on parabolic mirror and orthographic camera. The 3D point  $P(X,Y,Z)$  is projected on the mirror as point  $p_m(x_m, y_m, z_m)$  and on the image plan in  $p(x,y)$  (Figure 1).

According to the used projection model, the image projection  $p(x,y)$  of a 3D point  $P(X,Y,Z)$  can be defined by:

$$\begin{cases} x = \alpha_x \frac{h, X}{\sqrt{X^2 + Y^2 + Z^2 - Z}} + x_0 \\ y = \alpha_y \frac{h, Y}{\sqrt{X^2 + Y^2 + Z^2 - Z}} + y_0 \end{cases} \quad (3)$$

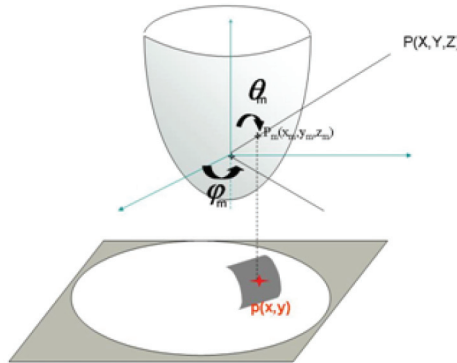
where  $\alpha_x$  (respectively  $\alpha_y$ ) is a scale in x direction (respectively y direction) between world coordinates and image coordinates.  $(x_0, y_0)$  are coordinates of a principal point which correspond to image coordinates of the projection of camera origin on the retina and  $h$  is the mirror parameter.

To simplify this modeling, we consider that the displacement components of 3D point  $\vec{D} = (d_x, d_y)$  are small and can be neglected compared to the 3D world coordinates of point P. Moreover, the scale in x direction and y direction will be considered equal to simplify equations.

Applying several algebraic manipulations, it leads to the following motion model equation:

$$\begin{cases} u = A(x - x_0)^2 + A(y - y_0)^2 + C \\ v = B(x - x_0)^2 + B(y - y_0)^2 + D \end{cases} \quad (4)$$

Figure 1. Projection model for parabolic mirror



Where the motion parameters means:

$$A = \frac{d_x}{2Zh\alpha}; B = \frac{d_y}{2Zh\alpha}; C = \frac{\alpha hd_x}{2Z}; \\ D = \frac{\alpha hd_y}{2Z}$$

Following to the motion model (eq. 4), the translation of 3D point in space describes a circle in image plane and depends on the position of point in image. The parameters of the motion depend on  $Z$ ,  $h$ ,  $\alpha$ , and displacement ( $d_x, d_y$ ). This motion model will be used to constraint the motion around the point  $(x, y)$  by searching  $\theta = (A, B, C, D)$  solution of equation. (5). To solve the over-determined system of equations, the least squares method is used.

$$\vec{V}(x, y) \arg \min_{\theta} \sum_{x', y' \in \vartheta_{x,y}} \left[ \frac{\partial I}{\partial x'} \cdot (A(x' - x_0)^2 + B(y' - y_0)^2 + C) + \frac{\partial I}{\partial y} \cdot (B(x' - x_0)^2 + B(y' - y_0)^2 + D) + \frac{\partial I}{\partial t} \right]^2 \quad (5)$$

## 1.2. Adapted Neighborhood

It is known that rectangular windows usually used for cameras with perspective projections are not appropriate for catadioptric cameras

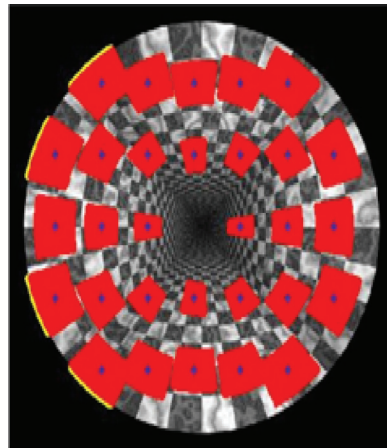
with a non linear projection. We propose thus an adapted neighborhood using the shape of the parabolic mirror. Each point in image presented with a Cartesian coordinates  $p=(x,y)$  is projected to the mirror point represented in spherical coordinates as  $p_m = (r, \theta_m, \varphi_m)$ , where  $\theta_m$  denotes the elevation,  $\varphi_m$  the azimuth and  $r$  is the distance of the point from the effective view point (Figure 1). The desired neighborhood is obtained by selecting image points in interval fixed on a range of elevation  $d\theta$  and azimuth  $d\varphi$  to determine the nearest mirror point to the image point  $p=(x,y)$ . Let  $p_{mt} = (r_t, \theta_{mt}, \varphi_{mt})$  be the spherical coordinates of the projection image point  $p_i=(x_i, y_i)$  in the mirror. The adapted neighborhood  $\vartheta_{x,y}$  is defined as follows:

$$(x_t, y_t) \in \vartheta_{x,y} \leftrightarrow |\theta_m - \theta_{mt}| < d\theta \text{ and } |\varphi_m - \varphi_{mt}| < d\varphi \quad (6)$$

The adapted neighborhood will be bigger if the point is close to the mirror's periphery and smaller if the point is close to the image center. This is a proof that the neighborhood is adapted to the resolution of these images since its size changes (Figure 2).

We use an adapted method based on new constraint to obtain the motion field in paraca-

Figure 2. An adapted neighborhood used for recovering optic flow



dioptric images. This new constraint is based on motion model, defined in equation. (4) and which is appropriate to the geometry of our image formation, and applied in adapted neighborhood  $\vartheta_{x,y}$  solve equation. (5). The solution will be used as flow field to estimate the camera motion.

## 2. EGOMOTION ESTIMATION FROM MOTION FIELD ON THE SPHERE

One of the applications of the optical flow is the estimation of the 3D motion of the camera starting from the 2D motion filed in the image. We start by computing the image motion with a sequence of omnidirectional images using our proposed adapted method described in previous section. Then, the image motion is mapped to the surface of a unit sphere, as if the camera had a truly spherical retina (Figure 3). This mapping is performed by means of determining the Jacobian of the transformation between spherical projection model and the image formation model of a paracatadioptric camera. Once the image motion vectors are mapped to the unit sphere, the egomotion algorithms used in perspective images must be adapted to the spherical projec-

tion model. We use the Brus-Horn's method to determine the translation direction and rotation angle of the catadioptric camera using spherical motion field.

### 2.1. Projection Model on the Sphere

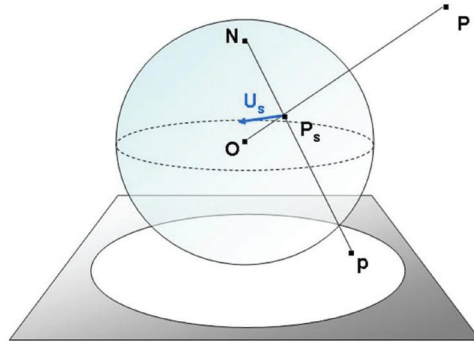
The rigid motion of a scene point P relative to a moving camera can be described as follows:

$$P = -T - \Omega \times P \quad (7)$$

Where T is the translation vector and  $\Omega$  is the rotation vector of the camera.

Let  $P_s(X_s, Y_s, Z_s) = P_s(\theta, \varphi)$  be a point on the sphere. A spherical perspective projection maps scenes point P(X, Y, Z) on 3D surface of unit sphere using eq. (8).

$$\begin{cases} X_s = \frac{x}{\sqrt{X^2 + Y^2 + Z^2}} \\ Y_s = \frac{y}{\sqrt{X^2 + Y^2 + Z^2}} \\ Z_s = \frac{z}{\sqrt{X^2 + Y^2 + Z^2}} \end{cases} \quad (8)$$

*Figure 3. A spherical perspective projection*

In spherical coordinates, where  $\theta$  is the polar angle between (PO) and the Z-axis and  $\varphi$  is the azimuth angle, we have:

$$\varphi = \arctan \frac{y}{x}; \quad \theta = 2 \arctan \frac{\sqrt{x^2 + y^2}}{h}$$

Where  $h$  is the radius of the parabolic mirror in the x-y plane.

Now we need to map motion field defined on omnidirectional image  $V=(u,v)$  on the sphere. It will be noted  $U_s(U_x, U_y, U_z)$ . Gluckman and Nayar (1998) have defined a transformation to do this efficiently. Their proposed method combines a transformation between points in the image to points on the sphere and the jacobian of this transformation. We consider the case of parabolic mirror, this transformation reads:

$$U_s = SJ \begin{pmatrix} u \\ v \end{pmatrix} \quad (9)$$

Where:

$$S = \begin{pmatrix} \frac{\partial x}{\partial \theta} & \frac{\partial x}{\partial \varphi} \\ \frac{\partial y}{\partial \theta} & \frac{\partial y}{\partial \varphi} \\ \frac{\partial z}{\partial \theta} & \frac{\partial z}{\partial \varphi} \end{pmatrix} = \begin{pmatrix} \cos \theta \cos \varphi & -\sin \theta \sin \varphi \\ \cos \theta \sin \varphi & \sin \theta \cos \varphi \\ -\sin \theta & 0 \end{pmatrix}$$

$$\text{And} \\ I = \begin{pmatrix} \frac{\partial \theta}{\partial x} & \frac{\partial \theta}{\partial y} \\ \frac{\partial \varphi}{\partial x} & \frac{\partial \varphi}{\partial y} \end{pmatrix} = \begin{pmatrix} \frac{2hx}{\sqrt{y^2 + x^2}(h^2 + y^2 + x^2)} & \frac{2hy}{\sqrt{y^2 + x^2}(h^2 + y^2 + x^2)} \\ -\frac{y}{y^2 + x^2} & \frac{y}{y^2 + x^2} \end{pmatrix}$$

## 2.2. Egomotion Estimation on the Sphere

We define our egomotion estimation starting with optical flow field mapped to sphere. For this reason the equation of egomotion estimation, described by Bruss and Horn (1983) in perspective case, must be rewritten on the sphere in function of vector velocities and points on the sphere.

Using a spherical projection of the scene point  $P$ , the equation (10) can be obtained taking the derivatives with respect to time in eq. (8) and substituting the results in eq. (7). We obtain the velocity vector of a point  $P_s(X_s, Y_s, Z_s)$  on the unit sphere given in the following equation:

$$U_s = \frac{1}{\|p\|} ((T, P_s)P_s - T) - \Omega \times P_s \quad (10)$$

Bruss and Horn (1983) applied a simple algebraic manipulation to remove the depth term in the equivalent of eq. (10) in perspective case. They obtained a bilinear constraint on  $T$  and  $\Omega$  for each point in the perspective image. In the same way, and for the spherical image, Gluckman and Nayar (1998) removed the depth of point  $P_s$  by using epipolar constraint. The equation (10) becomes:

$$T \cdot (P_s \times (U_s + (\Omega x P_s))) = 0 \quad (11)$$

Taking a number of velocity vectors  $U_s$  at points  $P_s$  on the sphere, the estimation of ego-motion can be realized from eq. (11) for combined camera motion and a pure translation motion. In the case of a pure rotation, eq. (11) cannot be used since translation is null. We describe below the full algorithm used in our method to get the direction of translation and rotation angle of the catadioptric camera. Note that it requires knowledge about the type of camera motion.

In practice, we proceed along the following steps:

1. Estimate the optical flow on the image:

For each point on the image do:

- Determine the adapted neighborhood using eq. (6).
- Use the motion model to constraint the optical flow equation (4).
- Apply least square estimation to solve the over-determined system using eq. (5).

2. Map image flow field on the sphere:

Map the optical flow field recovered in the image at step (1) on the unit sphere using eq. (9)

3. Estimate rotation angle and direction of translation:

If the camera motion is about a combined motion or pure translation motion:

- Initialize the translation vector  $T$ ,
- Estimate  $\Omega$  with least squares as function of  $T$
- The result is replaced in equation. (11), and gives a non-linear constraint on  $T$  which can be solved using a non-linear minimization method (Levenberg & Marquart (1963)) considering  $\|T\| = 1$ .
- Use the calculated translation vector to recover  $\Omega$ .

else

Apply least square of  $\Omega$  directly in equation. (10) as the depth term is removed with a null translation.

In addition, the case of pure translation can be treated in two different ways:

1. Use the general algorithm of non - linear minimization and solve the equation. (11).

Use direct solution of equation. (12) for a pure translation.

$$T \cdot (P_s \times U_s) = 0 \quad (12)$$

### 3. EXPERIMENTS AND RESULTS

We use the following method for recovering the motion field to compute egomotion from sequences of real and synthetic images using parabolic mirror. Let  $T$  and  $\Omega$  be the known translation and rotation applied to the camera and  $\hat{T}$  and  $\hat{\Omega}$  are the estimated rotation and translation. As translation can only be recovered up to a scale factor, only its direction is considered. The error in rotation and direction of translation are calculated as:

$$e_r = \Omega - \hat{\Omega}; e_t = a \cos(T, \hat{T})$$

We use this error measurement in order to compare the egomotion estimation computed

using the adapted method which is described bellow with that using classical method of Lucas and Kanade (1981). We give here detail of our simulations and obtained results.

### 3.1. Synthetic Sequences

The synthetic images have been generated with POVRAY. A virtual parabolic camera observes four textured planes approximatively separated by 100cm. POVRAY generated images of \$500\*500\$ pixels. For all sequences, the intrinsic parameters are fixed on  $\alpha=100$  and  $h=2.3$ . An example of synthetic images is illustrated in Figure 4. From the images set, optical flow field is computed using an adapted and classical method and mapped to a sphere. Then the direction of translation and rotation vector is derived from image velocity applying several kind of camera motion: Translation, rotation and combined motion (rotation and translation). We give bellow the two motion fields (classical and adapted one) used to estimate egomotion and error values in the translation and rotation corresponding to each experiment.

The first sequence results from a pure translation of the camera using 2cm along the X-axis. Figure 5 depicts the optical flow field obtained with this movement using the proposed method compared with that obtained using the traditional method. We also illustrate the motion field obtained with the known information about the scene (the ground truth).

The second experiment uses a camera in rotation around the Z-axis. For this case of rotational movement, the estimation with least squares is applied using the equation. (10) since the translation is null. The motion fields are illustrated in Figure 6 and the error obtained for the estimation of the camera rotation is indicated in Table 1.

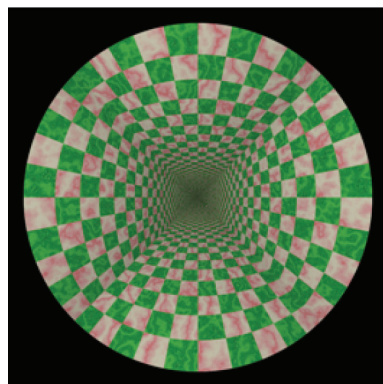
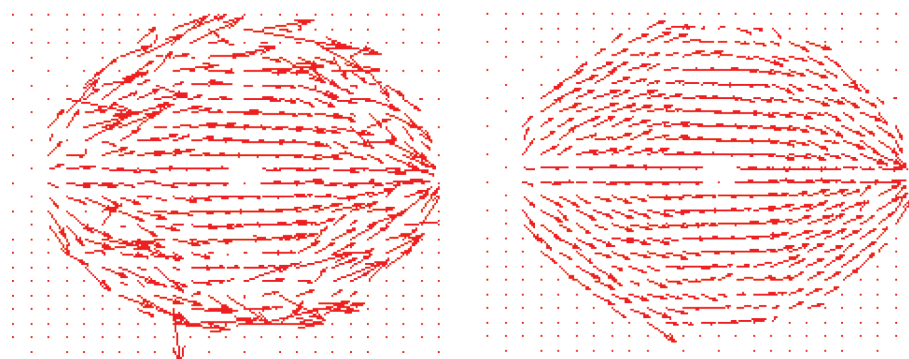
The third experiment presents a more complex movement which combines a translation 3cm along X-axis of the camera followed by a rotation with an angle =  $2^\circ$  around the Z-axis.

These fields are used to estimate the direction of translation and rotation angle of the cameras applying the algorithm described in section. (2.2). Note that we must know a nature of camera motion to choose the equation that must be used. The errors obtained for all previous experiments are summarized in Table 1.

### 3.2. Real Sequences

The sequences are obtained using a camera which is mounted on a mobile robot and moves on a plane perpendicular to its optical axis. The camera is a SONY DFW-SX910. We obtain an image of 1280\*960 pixels. The camera is calibrated using the Omnidirectional Calibration Toolbox (Mei & Rives, 2007). We obtained  $u_0=632,66$ ,  $v_0=459,02$  and  $h=0.86$ . To maintain the assumption used to get the motion model, we assume that  $\alpha_x = \alpha_y = 480,62$ .

Like in synthetic case, we will use three kind of camera motion. The first experiments consist on movement of mobile robot with translation along the X-Axis. The 2D motion fields obtained using the two methods are shown in the Figure 8 with the used images. Second experiments consider mobile robot in rotation around the Z-axis. The 2D motion fields obtained using the two methods (Lucas-Kanade's method and our adapted method) are shown in the Figure 9 with the used images. Last experiments consider a combined motion of mobile robot in the scene environment. The 2D motion fields obtained using the two methods are shown in Figure 10 with the used images. The camera used on the three experiments is calibrated. Using the model describing the mobile robot displacement, we need to know the direction of translation observed for the applied movement, and the rotation angle taken from odometry process. We use the knowledge about the camera motion used in these experiments to compare the errors on translation and rotation using classical and our adapted motion fields. These errors are given in Table 2.

*Figure 4. A synthetic image from image sequences results from virtual camera**Figure 5. Optical flow field for pure translation motion, virtual camera was translated 2cm along X-axis. Left: classical field. Right: Adapted field.**Table 1. Errors on translation and rotation estimated from motion field in synthetic images*

Motion	Errors	Classical method	Adapted method
Translation	Translation error	1.76°	0.57°
Rotation	Rotation error	0.60	0.51
Combined motion	Rotation error Translation error	1.05 3.29°	0.98 1.27°

*Table 2. Errors on translation and rotation estimated from motion field in real images*

Motion	Errors	Classical method	Adapted method
Translation	Translation error	6.40°	0.39°
Rotation	Rotation error	0.22	0.11
Combined motion	Rotation error Translation error	1.99 13.29°	1.93 7.91°

*Figure 6. Optical flow field for pure rotation motion, virtual camera was rotate along Z-axis with 2°. Left: classical field. Right: Adapted field.*

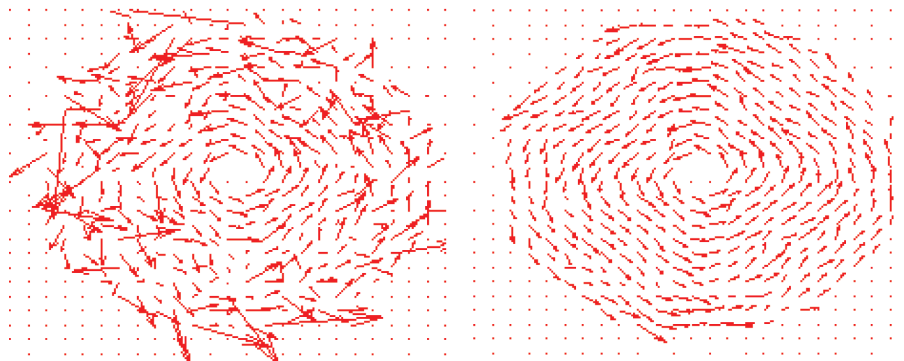
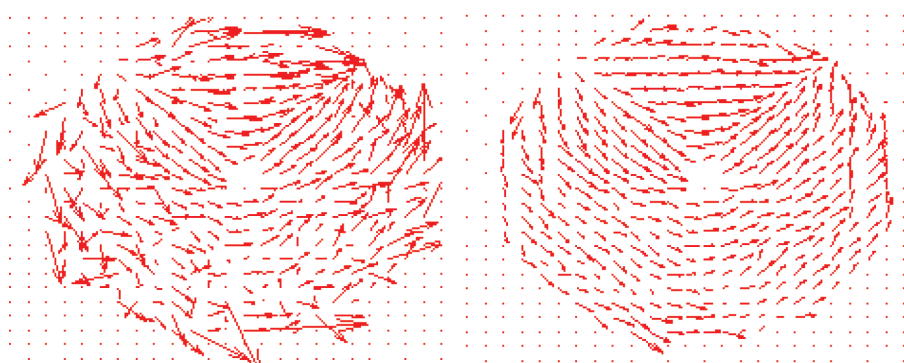


*Figure 7. Optical flow field for combined motion: rotation 2° around Z-axis and translation 3cm along X-axis. Left: classical field. Right: Adapted field.*



From the vector flow field estimated with the two approaches, we can observe that the adapted one is more appropriate to omnidirectional images. It also considers the different resolution existing in catadioptric image. The egomotion estimation with this adapted field allows more correct motion analysis as it is shown in errors values compared in different kind of smoothed camera motions in real and synthetic images. Since equation (11) is not general, it remain difficult to choose which model of motion must be used for the egomotion estimation if no information about the camera motion is available, especially in a pure rotation case. It is interesting to combine the equations given by Bruss and Horn (1983) to

get general model of egomotion estimation more suitable for an arbitrary camera motion.

#### 4. CONCLUSION

Recent development in omnidirectional imaging system provides varieties of sensors with large field of view. The images, provided with this kind of sensor, allow overcoming the limitation presented in planar-projection imagery in order to address the motion estimation problem. Previous research related to motion estimation from omnidirectional images uses image motion fields computed using classical method developed for perspective images. This work suggests using an adapted motion field to com-

Figure 8. Optical flow field in real images using pure translation motion. Left: classical field. Right: Adapted field.

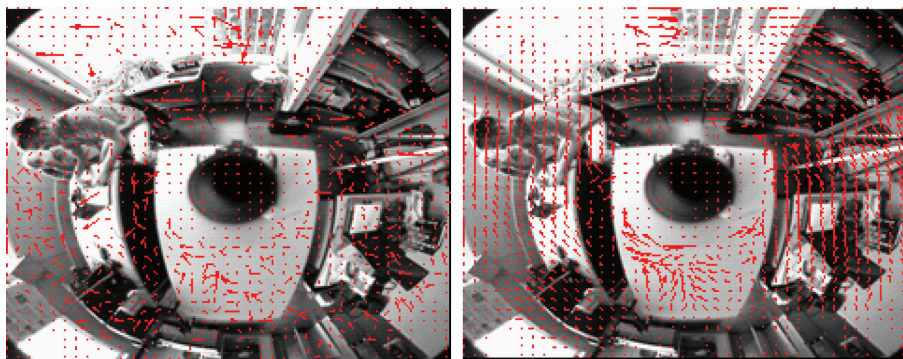


Figure 9. Optical flow field in real images using pure rotation motion. Left: classical field. Right: Adapted field.

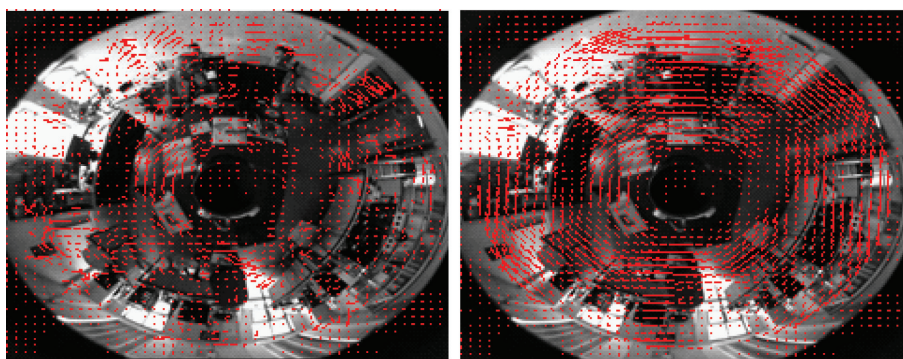
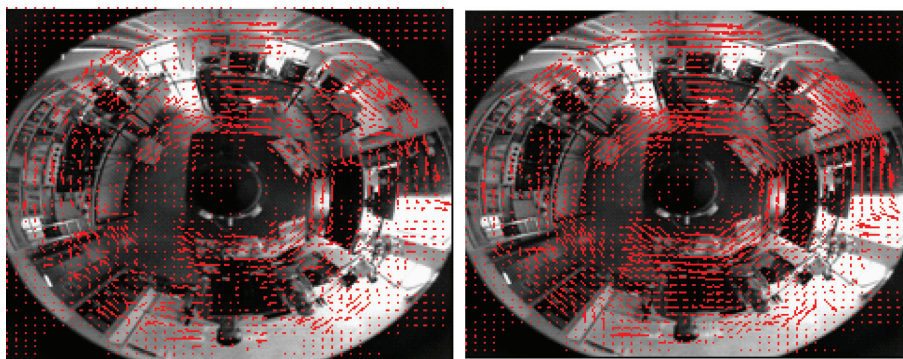


Figure 10. Optical flow field in real images using combined motion. Left: classical field. Right: Adapted field.



pute egomotion from paracatadioptric images. The simulation results show that adapted motion field generates accurate translation and rotation estimates for a wide range of camera motions.

## ACKNOWLEDGMENT

This work is supported by the project MA/07/174, PAI: VOLUBILIS.

## REFERENCES

- Bruss, A., & Horn, B. K. P. (1983). Passive navigation. *Journal of Computer Vision . Graphics and Image Processing*, 21, 276–283.
- Bunschoten, R., & Kroese, B. (2003). Visual odometry from an omnidirectional vision system. In . *Proceedings of the IEEE International Conference on Robotics and Automation*, 1, 577–583.
- Gandhi, T., & Trivedi, M. (2005). Parametric egomotion estimation for vehicle surround analysis using an omnidirectional camera. *Journal of Machine Vision and Applications*, 16(2), 85–95. doi:10.1007/s00138-004-0168-z
- Geyer, C., & Daniilidis, K. (2000). A unifying theory for central panoramic systems and practical implications. In *Proceedings of the 6th European Conference on Computer Vision- Part 2* (pp. 445-461).
- Gluckman, J., & Nayar, S. K. (1998). Ego-motion and omnidirectional cameras. In *Proceedings of the 6th International Conference on Computer Vision* (pp. 999-1005).
- Kim, J., & Suga, Y. (2007). An omnidirectional vision-based moving obstacle detection in mobile robot. *International Journal of Control Automation and Systems*, 5(6), 663–673.
- Lee, J. W., You, S., & Neumann, U. (2000). Large motion estimation for omnidirectional vision. In *Proceedings of the IEEE Workshop on Omnidirectional Vision* (p. 161).
- Lim, J., & Barnes, N. (2008). Directions of egomotion from antipodal points. In *Proceedings of Conference on Computer Vision and Pattern Recognition* (pp. 1-8).
- Lim, J., & Barnes, N. (2009). Estimation of the epipole using optical flow at antipodal points. In *Proceedings of the 11th International Conference on Computer Vision* (pp. 1-6).
- Lucas, B., & Kanade, T. (1981). An iterative image registration technique with an application to stereo vision. In *Proceedings of the 7th Internatioanl Joint Conference on Artificial Intelligence* (Vol. 2, pp. 674-679).
- Marquardt, D. W. (1963). An algorithm for least-squares estimation of nonlinear parameters. *Journal of the Society for Industrial and Applied Mathematics*, 11(2), 431–441. doi:10.1137/0111030
- Mei, C., & Rives, P. (2007). Single view point omnidirectional camera calibration from planar grids. In *Proceedings of the IEEE International Conference on Robotics and Automation* (pp. 3945-3950).
- Radgui, A., Demonceaux, C., Mouaddib, E., Aboutajdine, D., & Rziza, M. (2008, September). *An adapted Lucas-Kanade's method for optical flow estimation in catadioptric images*. Paper presented at the Eighth Workshop on Omnidirectional Vision and Camera Networks, and Non-Classical Cameras.
- Shakernia, O., Vidal, R., & Sastry, S. (2003). Omnidirectional egomotion estimation from back-projection flow. In *Proceedings of the IEEE Conference on Computer Vision and Pattern Recognition Workshop* (p. 82).
- Svoboda, T., Pajdla, T., & Hlavac, V. (1998). *Motion estimation using central panoramic cameras*. Paper presented at the IEEE Conference on Intelligent Vehicles, Stuttgart, Germany.
- Thanh, T. N., Nagahara, H., Sagawa, R., Mukaigawa, Y., Yachida, M., & Yagi, Y. (2008). Robust and real-time egomotion estimation using a compound omnidirectional sensor. In *Proceedings of the IEEE International Conference on Robotics and Automation* (pp.492-497).
- Tian, T. Y., Tomasi, C., & Heeger, D. J. (1996). Comparison of approaches to egomotion computation. In *Proceedings of the IEEE Conference on Computer Vision and Pattern Recognition* (pp. 315-320).
- Vassallo, R. F., Santos-Victor, J., & Schneebeli, H. J. (2002). A general approach for egomotion estimation with omnidi- rectional images. In *Proceedings of the IEEE Workshop on Omnidirectional Vision* (pp.97-103).
- Wang, M. L., Huang, C. C., & Lin, H. Y. (2006). An intelligent surveillance system based on an omnidirectional vision sensor. In *Proceedings of the IEEE Conference on Cybernetics and Intelligent Systems* (pp. 1-6).

- Winters, N., Gaspar, J., Lacey, G., & Santos-Victor, J. (2000). Omni-directional vision for robot navigation. In *Proceedings of the IEEE Workshop on Omnidirectional Vision* (pp. 21-28).
- Yoshizaki, W., Mochizuki, Y., Ohnishi, N., & Imiya, A. (2008, September). *Free space detection from catadioptric omnidirectional images for visual navigation using optical flow*. Paper presented at the 8th Workshop on Omnidirectional Vision, Camera Networks, and Non-Classical Cameras.